Geomechanics and Engineering, *Vol. 7, No. 4 (2014) 355-374*
DOI: http://dx.doi.org/10.12989/gae.2014.7.4.355

Plane strain consolidation of a compressible clay stratum by surface loads

Sunita Rani [*1], Manoj Puri [1a] and Sarva Jit Singh [2b]

[1] *Department of Mathematics, Guru Jambheshwar University of Science and Technology,Hisar-125001, India*
[2] *Indian National Science Academy, New Delhi-110002, India*

(*Received August 27, 2013, Revised April 11, 2014, Accepted June 09, 2014*)

Abstract. An analytical solution of the fully coupled system of equations governing the plane strain deformation of a poroelastic medium with anisotropic permeability and compressible fluid and solid constituents is obtained. This solution is used to study the consolidation of a poroelastic clay layer with free permeable surface resting on a rough-rigid permeable or impermeable base. The stresses and the pore pressure are taken as the basic state variables. Displacements are obtained by integrating the coupled constitutive relations. The case of normal surface loading is discussed in detail. The solution is obtained in the Laplace-Fourier domain. Two integrations are required to obtain the solution in the space-time domain which are evaluated numerically for normal strip loading. Consolidation of the clay layer and diffusion of pore pressure is studied for both the bases. It is found that the time settlement is accelerated by the permeability of the base. Initially, the pore pressure is not affected by the permeability of the base, but has a significant effect, as we move towards the bottom of the layer. Also, anisotropy in permeability and compressibilities of constituents of the poroelastic medium have a significant effect on the consolidation of the clay layer.

Keywords: anisotropic permeability; clay stratum; compressible constituents; normal strip loading; plane strain; poroelastic

1. Introduction

Biot's theory of linear poroelasticity has been used extensively to study the consolidation of a layered poroelastic medium. Some researchers have included the anisotropy in hydraulic permeability in the study of the deformation of a porous medium e.g., Booker and Randolph (1984), Booker and Carter (1986, 1987a, b), Ganbe and Kurashige (2001), Taguchi and Kurashige (2002), Chen (2004, 2005), Chen and Gallipoli (2004), Singh *et al.* (2007), Ai and Wang (2008), Ai and Wu (2009), Rani *et al.* (2011) etc.

Booker and Randolph (1984) discussed the consolidation of a poroelastic half-space with cross anisotropic deformation and flow properties subjected to surface loading assuming the fluid and solid constituents incompressible. Chen (2004) studied the consolidation of a multilayered

*Corresponding author, Professor Sunita Rani, E-mail: s_b_rani@rediffmail.com
[a] E-mail: mnj243puri@gmail.com
[b] E-mail: s_j_singh@yahoo.com

http://www.techno-press.org/?journal=gae&subpage=7 ISSN: 2005-307X (Print), 2092-6219 (Online)

poroelastic half-space with anisotropic permeability assuming the pore fluid to be compressible and the solid skeleton to be incompressible. Chen (2005) obtained the response of a poroelastic half-space with transversely isotropic permeability and poroelasticity to a point sink taking both the fluid and solid constituents incompressible. Chen *et al.* (2005a, b) discussed axisymmetric consolidation of soil medium subjected to a uniform circular pressure on the ground surface. The poroelastic medium was assumed to be transversely isotropic in its elastic and hydraulic properties.

Singh *et al.* (2007) obtained an analytical solution of the system of equations governing the plane strain deformation of a poroelastic half-space with anisotropic permeability and compressible fluid and solid constituents. This solution has been used to study the consolidation of a half-space by surface loads. The corresponding three-dimensional problem of axisymmetric surface loads has been studied by Singh *et al.* (2009).

Ai and Wang (2008) obtained the axisymmetric consolidation of a soil layer using Laplace and Hankel transforms in terms of elements of the Thomson-Haskell matrix. Ai *et al.* (2008) solved Biot's three-dimensional consolidation problem for a saturated poroelastic multi-layered soil due to loading at an arbitrary interface in the Cartesian coordinate system using transfer matrix method. The corresponding problem of circular loading has been discussed by Ai *et al.* (2010a). Subsequently, Ai *et al.* (2010b) presented transfer matrix solutions to study the axisymmetric and non-axisymmetric consolidation of a multilayered soil under arbitrary loading.

Ai and Wu (2009) obtained a solution for plane strain consolidation of a soil layer with anisotropic permeability and incompressible fluid and solid constituents due to surface loads. The case of strip loading is discussed numerically. Kim and Mission (2011) formulated a finite difference solution for the one-dimensional consolidation in multilayered clay profiles using interface boundary relations in terms of infinitesimal strain. Rani *et al.* (2011) obtained an analytical solution of the fully coupled system of equations governing the axisymmetric quasi-static deformation of a poroelastic clay layer with anisotropic permeability and compressible fluid and solid constituents using Laplace-Hankel transforms. The case of normal disk loading is discussed in detail. Li *et al.* (2013) obtained an analytical solution in term of summation of infinite series for the consolidation within a finite rectangular poroelastic medium due to uniform normal loading using Fourier and Laplace transforms. Ai *et al.* (2013) obtained the solution for three dimensional consolidation of a multi-layered poroelastic medium with anisotropic permeability and compressible pore fluid using a transfer matrix approach.

The purpose of the present study is to investigate analytically and numerically the plane strain deformation of a clay layer resting on a rough-rigid permeable or impermeable base due to surface loading. Both the solid and the fluid constituents are compressible. The permeability in the vertical direction is taken different from the permeability in the horizontal direction. The case of normal strip loading is discussed in detail. Numerical computations are performed to study the effect of the anisotropy in permeability and compressibilities of fluid and solid constituents for two cases: a layer resting on a rough-rigid permeable base and a layer resting on a rough-rigid impermeable base. The present study may find applications in the consolidation process of clay layers due to surface loading. The theory developed is significant in the study of consolidation of a poroelastic layer which is mechanically isotropic but hydraulically anisotropic.

2. Basic equations

A homogeneous, isotropic, poroelastic medium can be characterized by four constitutive constants. Let these constants be the shear modulus (G), the drained Poisson's ratio (υ), the undrained Poisson's ratio (υ_u) and the Biot-Willis coefficient (α). For plane strain deformation of a poroelastic medium in the x_1x_3-plane, the displacement components in the solid skeleton are of the form

$$u_1 = u_1(x_1, x_3, t), \quad u_2 = 0, \quad u_3 = u_3(x_1, x_3, t) \tag{1}$$

Let σ_{ij} denote the total stress tensor in the fluid-infiltrated porous elastic material, ε_{ij} the corresponding strain tensor and p the excess fluid pore pressure. For plane strain, these quantities are related through the following coupled system of equations (Detournay and Cheng 1993) in which σ_{ij} and p are taken as the basic state variables.

2.1 Equations of equilibrium

$$\frac{\partial \sigma_{11}}{\partial x_1} + \frac{\partial \sigma_{13}}{\partial x_3} = 0, \quad \frac{\partial \sigma_{13}}{\partial x_1} + \frac{\partial \sigma_{33}}{\partial x_3} = 0 \tag{2}$$

2.2 Compatibility equation

$$\nabla^2(\sigma_{11} + \sigma_{33} + 2\eta p) = 0, \tag{3}$$

where

$$\eta = \frac{1-2\upsilon}{2(1-\upsilon)}\alpha \tag{4}$$

is the poroelastic stress coefficient.

2.3 Constitutive equations

$$2G\varepsilon_{11} = (1-\upsilon)\sigma_{11} - \upsilon\sigma_{33} + \alpha_0 p \tag{5}$$

$$2G\varepsilon_{33} = (1-\upsilon)\sigma_{33} - \upsilon\sigma_{11} + \alpha_0 p \tag{6}$$

$$2G\varepsilon_{13} = \sigma_{13}, \quad \varepsilon_{21} = \varepsilon_{22} = \varepsilon_{23} = 0 \tag{7}$$

$$\sigma_{22} = \upsilon(\sigma_{11} + \sigma_{33}) - \alpha_0 p, \quad \sigma_{21} = \sigma_{23} = 0 \tag{8}$$

where

$$\alpha_0 = (1-2\upsilon)\alpha \tag{9}$$

2.4 Darcy's law

According to Darcy's law of fluid flow in a poroelastic medium with anisotropic permeability

$$q_1 = -\chi_1 \partial p/\partial x_1 \quad q_2 = 0, \quad q_3 = -\chi_3 \partial p/\partial x_3 \tag{10}$$

where $\mathbf{q}$ is the fluid flux and χ_i is the Darcy conductivity in the x_i-direction.

2.5 Fluid diffusion equation

$$\frac{\partial}{\partial t}\left(\sigma_{11}+\sigma_{33}+\frac{\alpha_0}{\upsilon_u-\upsilon}p\right)=\frac{2G}{\alpha_0}\left(\chi_1\frac{\partial^2 p}{\partial x_1^2}+\chi_3\frac{\partial^2 p}{\partial x_3^2}\right) \tag{11}$$

Eq. (11) may be written in the form

$$\frac{\partial}{\partial t}\left(\sigma_{11}+\sigma_{33}+\frac{\alpha_0}{\upsilon_u-\upsilon}p\right)=\frac{\alpha_0(1-\upsilon_u)}{(1-\upsilon)(\upsilon_u-\upsilon)}\nabla_{13}^2 p \tag{12}$$

where

$$\nabla_{13}^2=c_1\frac{\partial^2}{\partial x_1^2}+c_3\frac{\partial^2}{\partial x_3^2} \tag{13}$$

and

$$c_i=\frac{2G(1-\upsilon)(\upsilon_u-\upsilon)}{\alpha_0^2(1-\upsilon_u)}\chi_i \quad (i=1,3) \tag{14}$$

is the hydraulic diffusivity.

Using Eqs. (5) and (6), Eq. (11) can be expressed in the form

$$\left(\chi_1\frac{\partial^2}{\partial x_1^2}+\chi_3\frac{\partial^2}{\partial x_3^2}\right)p=\frac{\partial}{\partial t}\left(\alpha\, div\, \boldsymbol{u}+\frac{p}{M}\right) \tag{15}$$

where

$$M=\frac{2G(\upsilon_u-\upsilon)}{\alpha^2(1-2\upsilon)(1-2\upsilon_u)} \tag{16}$$

is the Biot modulus.

3. Solution of the governing equations

The four unknowns σ_{11}, σ_{33}, σ_{13} and p are to be determined from the coupled system of the four Eqs. (2), (3) and (12). This system can be solved in terms of Biot's stress function F such that (Wang 2000)

$$\sigma_{11}=\frac{\partial^2 F}{\partial x_3^2},\quad \sigma_{33}=\frac{\partial^2 F}{\partial x_1^2},\quad \sigma_{13}=-\frac{\partial^2 F}{\partial x_1\partial x_3} \tag{17}$$

The equilibrium Eq. (2) are then identically satisfied. Eqs. (3), (12) and (17) yield

$$\nabla^2(\nabla^2 F+2\eta p)=0, \tag{18}$$

$$\frac{\partial}{\partial t}\left[\nabla^2 F+\frac{\alpha_0}{\upsilon_u-\upsilon}p\right]=\frac{\alpha_0(1-\upsilon_u)}{(1-\upsilon)(\upsilon_u-\upsilon)}\nabla_{13}^2 p \tag{19}$$

Eliminating F and p in turn, Eqs. (18) and (19) lead to the following decoupled equations

$$\left(\nabla_{13}^2 - \frac{\partial}{\partial t}\right)\nabla^2 p = 0, \tag{20}$$

$$\left(\nabla_{13}^2 - \frac{\partial}{\partial t}\right)\nabla^4 F = 0. \tag{21}$$

Taking the Laplace transform of Eqs. (20) and (21), we obtain

$$(\nabla_{13}^2 - s)\nabla^2 p = 0, \tag{22}$$

$$(\nabla_{13}^2 - s)\nabla^4 F = 0. \tag{23}$$

where now $p(x_1, x_3, t)$ and $F(x_1, x_3, s)$ denote the Laplace transform of (x_1, x_3, t) and $F(x_1, x_3, t)$, respectively and s denotes the Laplace transform variable.

A straightforward method of solving equations of the type Eqs. (22) and (23) has been given by Roeloffs (1988, Appendix) and Wang (2000, pp. 157-159). Thus, the general solution of Eq. (22) may be expressed in the form

$$p = p_1 + p_2, \tag{24a}$$

where

$$\nabla_{13}^2 p_1 - s p_1 = 0, \quad \nabla^2 p_2 = 0. \tag{24b}$$

Similarly, the general solution of Eq. (23) may be expressed in the form

$$F = F_1 + F_2, \tag{25a}$$

where

$$\nabla_{13}^2 F_1 - s F_1 = 0, \quad \nabla^4 F_2 = 0. \tag{25b}$$

Eqs. (24b) and (25b) can be solved by taking Fourier transform in the x_1 coordinate and then solving the resulting ordinary differential equations. We thus find that for the deformation of a homogeneous poroelastic clay stratum $0 \le z \le h$ by surface loads, suitable solutions of Eqs. (22) and (23) are of the form

$$p = \int_0^\infty \left[A_1 e^{-mz} + A_2 e^{-kz} + A_3 e^{mz} + A_4 e^{kz}\right]\begin{pmatrix}\sin kx \\ \cos kx\end{pmatrix} dk, \tag{26}$$

$$F = \int_0^\infty \left[B_1 e^{-mz} + (B_2 + B_3 kz)e^{-kz} + B_4 e^{mz} + (B_5 + B_6 kz)e^{kz}\right]\begin{pmatrix}\sin kx \\ \cos kx\end{pmatrix} dk, \tag{27}$$

where the arbitrary constants A_1, A_2, etc. may be functions of k, $x = x_1$, $z = x_3$ and

$$m = \left(\frac{c_1}{c_3}k^2 + \frac{s}{c_3}\right)^{1/2}. \tag{28}$$

Inserting the expressions for F and p from Eqs. (26) and (27) in Eq. (18), we find

$$B_1 = \frac{2\eta}{k^2 - m^2} A_1, \quad B_4 = \frac{2\eta}{k^2 - m^2} A_3. \tag{29}$$

Similarly, Eq. (20) implies

$$B_3 = \frac{\alpha_0 A_2}{2k^2(\upsilon_u - \upsilon)}\left[1 + \frac{(c_1 - c_3)(1-\upsilon_u)k^2}{(1-\upsilon)s}\right], \quad B_6 = -\frac{\alpha_0 A_4}{2k^2(\upsilon_u - \upsilon)}\left[1 + \frac{(c_1 - c_3)(1-\upsilon_u)k^2}{(1-\upsilon)s}\right]. \tag{30}$$

Eqs. (10), (17), (26) and (27) yield

$$q_1 = -\chi_1 \int_0^\infty \left[A_1 e^{-mz} + A_2 e^{-kz} + A_3 e^{mz} + A_4 e^{kz}\right]\begin{pmatrix} \cos kx \\ -\sin kx \end{pmatrix} k\, dk, \tag{31}$$

$$q_3 = \chi_3 \int_0^\infty \left[m(A_1 e^{-mz} - A_3 e^{mz}) + k(A_2 e^{-kz} - A_4 e^{kz})\right]\begin{pmatrix} \sin kx \\ \cos kx \end{pmatrix} dk, \tag{32}$$

$$\sigma_{11} = \int_0^\infty \left[m^2(B_1 e^{-mz} + B_4 e^{mz}) + k^2\left\{\left[B_2 + (kz-2)B_3\right]e^{-kz} + \left[B_5 + (kz+2)B_6\right]e^{kz}\right\}\right]\begin{pmatrix} \sin kx \\ \cos kx \end{pmatrix} dk, \tag{33}$$

$$\sigma_{33} = -\int_0^\infty \left[(B_1 e^{-mz} + B_4 e^{mz}) + (B_2 + B_3 kz)e^{-kz} + (B_5 + B_6 kz)e^{kz}\right]\begin{pmatrix} \sin kx \\ \cos kx \end{pmatrix} k^2\, dk, \tag{34}$$

$$\sigma_{13} = \int_0^\infty \left[m(B_1 e^{-mz} - B_4 e^{mz}) + k\left\{\left[B_2 + (kz-1)B_3\right]e^{-kz} - \left[B_5 + (kz+1)B_6\right]e^{kz}\right\}\right]\begin{pmatrix} \cos kx \\ -\sin kx \end{pmatrix} k\, dk. \tag{35}$$

Corresponding to the stresses given by Eqs. (33)-(35), the displacements are found by integrating the constitutive Eqs. (5) to (7). We find

$$\begin{aligned} 2Gu_1 = -\int_0^\infty \Bigg[& B_1 e^{-mz} + B_4 e^{mz} + \left\{B_2 + B_3(kz + 2\upsilon - 2) + \frac{\alpha_0}{k^2} A_2\right\} e^{-kz} \\ & + \left\{B_5 + B_6(kz - 2\upsilon + 2) + \frac{\alpha_0}{k^2} A_4\right\} e^{kz}\Bigg]\begin{pmatrix} \cos kx \\ -\sin kx \end{pmatrix} k\, dk, \end{aligned} \tag{36}$$

$$\begin{aligned} 2Gu_3 = \int_0^\infty \Bigg[& m(B_1 e^{-mz} - B_4 e^{mz}) + \left\{B_2 + B_3(1 - 2\upsilon + kz) - \frac{\alpha_0}{k^2} A_2\right\} k\, e^{-kz} \\ & - \left\{B_5 + B_6(1 - 2\upsilon - kz) + \frac{\alpha_0}{k^2} A_4\right\} k\, e^{kz}\Bigg]\begin{pmatrix} \sin kx \\ \cos kx \end{pmatrix} dk. \end{aligned} \tag{37}$$

In deriving Eqs. (36)-(37), the relation Eq. (29) has been used. Eqs. (26) and (31) to Eq. (37) can be used to solve analytically the problem of the deformation of a homogeneous poroelastic clay stratum possessing anisotropic permeability and compressible constituents. The constants A_2, B_1, B_2 etc. are to be determined from the boundary conditions. As an example, we solve the problem of 2-D surface loads in the next section.

4. Surface loads

A normal load $(\sigma_{33})_0$ is applied on the surface $z = 0$ of the poroelastic clay stratum $0 \le z \le h$ overlying a rough-rigid base (Fig. 1). We assume that the boundary $z = 0$ is permeable, but the lower boundary $z = h$ may be permeable or impermeable. We consider both the cases: Case I, when the base $z = h$ is permeable and Case II, when the base $z = h$ is impermeable. The boundary conditions yield

$$\sigma_{13} = 0, \quad \sigma_{33} = (\sigma_{33})_0, \quad p = 0 \qquad \text{at } z = 0, \tag{38}$$

and

$$u_1 = u_3 = p = 0 \qquad \text{at } z = h \tag{39}$$

for case I, and

$$u_1 = u_3 = q_3 = 0 \qquad \text{at } z = h \tag{40}$$

for case II. Let

$$(\sigma_{33})_0 = \int_0^\infty N_0 \begin{pmatrix} \sin kx \\ \cos kx \end{pmatrix} k\, dk. \tag{41}$$

Eqs. (26), (32) and (34) to (41) yield six equations in six unknowns (A_1, A_2, A_3, A_4, B_2, B_5). Explicit expressions for these unknowns are given in the Appendix for Case I: Permeable base and

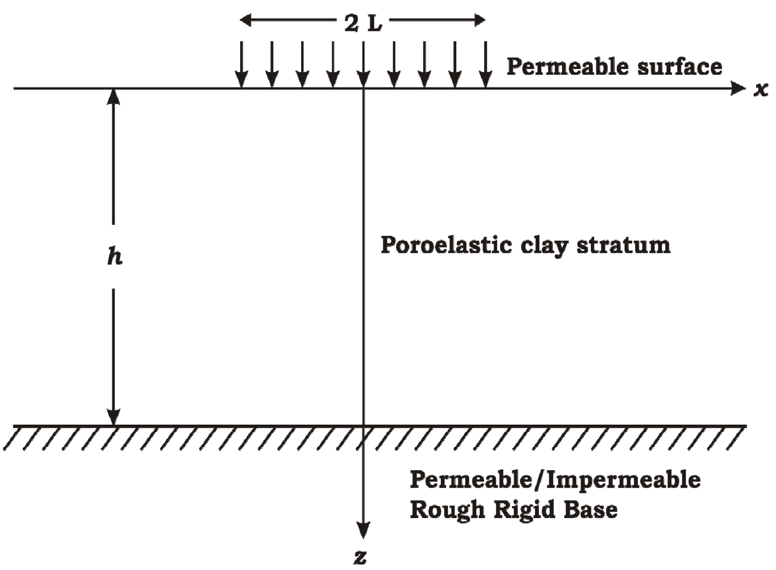

Fig. 1 Poroelastic clay stratum of thickness h with permeable free surface resting on a rough rigid permeable or impermeable base

Case II: Impermeable base, respectively.

Substituting the values of A_1, A_2, etc. in Eqs. (26) and (31) to (37), we get the integral expressions for the pore pressure, fluid flux, stresses and displacements. These integrals cannot be solved analytically. One has to resort to numerical integration.

5. Normal strip loading

Consider a strip $-L \le x \le L$ of infinite length in the y-direction on the surface. Let a normal load σ_0 per unit length acting in the positive z-direction be uniformly distributed over this strip. We have (Singh and Rani 2006)

$$(\sigma_{33})_0 = -\frac{\sigma_0}{\pi}\int_0^\infty \cos kx \frac{\sin kL}{kL}\, dk \tag{42}$$

for $z = 0$. Comparing Eqs. (41) and (42), we have

$$N_0 = -\frac{\sigma_0}{\pi k}\left(\frac{\sin kL}{kL}\right) \tag{43}$$

and the lower solution in Eqs. (31) to (37) is to be chosen. Inserting the values of constants, A_1, A_2, etc. from the Appendix into Eqs. (26) and (32)-(37), we get the expressions for the pore pressure, fluid flux, stresses and displacements at any point of the stratum caused by strip loading for Case I: Permeable base and Case II: Impermeable base, respectively. We have verified that, as the depth h of the stratum tends to ∞, the integral expressions coincide with the corresponding results of a poroelastic half-space with anisotropic permeability and compressible constituents given by Singh *et al.* (2007). Explicit expressions for the Laplace transform of pore pressure $p(x, z, s)$ and the vertical (down) displacement at the original $u_3(0, 0, s)$ are found to be

Case I: Permeable base

$$\begin{aligned}
p\,(x,z,s) = -\frac{\sigma_0}{\pi\eta s}\int_0^\infty \Big[\Big\{ & 2(m\beta_5+\beta_4+\beta_1)\,e^{kh} - 2(m\beta_5-\beta_4+\beta_2)\,e^{-kh} - 2(k\beta_5+\beta_4)\,e^{mh} \\
& -\big[\beta_6+(m-k)\beta_5\big]e^{(m+2k)h} - \big[\beta_6-(m+k)\beta_5\big]e^{(m-2k)h}\Big\}e^{-mz} \\
& -\Big\{2m\beta_5(3e^{kh}+e^{-kh}) - \big[(\beta_4-\beta_1-\beta_2)+(3m+k)\beta_5\big]e^{mh} \\
& -\big[(\beta_4-\beta_1-\beta_2)-(3m-k)\beta_5\big]e^{-mh} - \big[\beta_6+(m-k)\beta_5\big]e^{(m+2k)h} \\
& +\big[\beta_6-(m+k)\beta_5\big]e^{-(m-2k)h}\Big\}e^{-kz} + \Big\{2(m\beta_5-\beta_4-\beta_1)\,e^{kh} - 2(m\beta_5+\beta_4-\beta_2)\,e^{-kh} \\
& +2(k\beta_5+\beta_4)\,e^{-mh} + \big[\beta_6-(m+k)\beta_5\big]e^{-(m-2k)h} + \big[\beta_6+(m-k)\beta_5\big]e^{-(m+2k)h}\Big\}e^{mz} \\
& +\Big\{2m\beta_5(e^{kh}+3e^{-kh}) + \big[(\beta_1+\beta_2+\beta_4)-(3m-k)\beta_5\big]e^{mh} \\
& -\big[(\beta_1+\beta_2+\beta_4)+(3m+k)\beta_5\big]e^{-mh} + \big[\beta_6-(m+k)\beta_5\big]e^{(m-2k)h} \\
& -\big[\beta_6+(m-k)\beta_5\big]e^{-(m+2k)h}\Big\}e^{kz}\Big]\frac{\sin kL \cos kx}{kLD}\,dk
\end{aligned} \tag{44}$$

$$u_3(0,0,s)=\frac{\sigma_0}{G\pi s}\int_0^\infty\left[8m\beta_5\cosh kh+4\beta_4 kh\sinh mh-6m\beta_5\cosh mh-\{\beta_6+(m-k)\beta_5\}\right.$$
$$\left.\times\cosh(m+2k)h+\{\beta_6-(m+k)\beta_5\}\cosh(m-2k)h\right]\frac{(\beta_4-\beta_3)\sin kL}{k^2LD}dk. \tag{45}$$

Case II: Impermeable base

$$p\,(x,z,s)=-\frac{\sigma_0}{\pi\eta s}\int_0^\infty\Big[\Big\{-2k(m\beta_5+\beta_2)\,e^{kh}-2k(m\beta_5+\beta_1)\,e^{-kh}+2m(k\beta_5+\beta_4)\,e^{mh}$$
$$+\left[m\beta_6+k(m-k)\beta_5\right]e^{(m+2k)h}+\left[m\beta_6+k(m+k)\beta_5\right]e^{(m-2k)h}\Big\}e^{-mz}$$
$$+\Big\{2mk\beta_5(3e^{kh}-e^{-kh})+\left[m(\beta_1+\beta_2-\beta_4)-(mk+k^2+2m^2)\beta_5\right]e^{mh}$$
$$+\left[m(\beta_1+\beta_2-\beta_4)-(mk-k^2-2m^2)\beta_5\right]e^{-mh}-\left[m\beta_6+k(m-k)\beta_5\right]e^{(m+2k)h}$$
$$-\left[m\beta_6+k(m+k)\beta_5\right]e^{-(m-2k)h}\Big\}e^{-kz}+\Big\{2k(\beta_2-m\beta_5)\,e^{kh}+2k(\beta_1-m\beta_5)\,e^{-kh} \tag{46}$$
$$+2m(\beta_4+k\beta_5)\,e^{-mh}+m\left[\beta_6+k(m+k)\beta_5\right]e^{-(m-2k)h}$$
$$+\left[m\beta_6+k(m-k)\beta_5\right]e^{-(m+2k)h}\Big\}e^{mz}+\Big\{2mk\beta_5(3e^{-kh}-e^{kh})$$
$$-\left[m(\beta_1+\beta_2+\beta_4)+(mk-k^2-2m^2)\beta_5\right]e^{mh}$$
$$-\left[m(\beta_1+\beta_2+\beta_4)+(mk+k^2+2m^2)\beta_5\right]e^{-mh}$$
$$-\left[m\beta_6+k(m+k)\beta_5\right]e^{(m-2k)h}-\left[m\beta_6+k(m-k)\beta_5\right]e^{-(m+2k)h}\Big\}e^{kz}\Big]\frac{\sin kL\cos kx}{kLD'}dk,$$

$$u_3(0,0,s)=\frac{\sigma_0}{\pi G s}\int_0^\infty\Big[-8mk\beta_5\sinh kh+2\beta_5(k^2+2m^2)\sinh mh-4mkh\beta_4\cosh mh$$
$$+\{m\beta_6+k(m-k)\beta_5\}\sinh(m+2k)h-\{m\beta_6+k(m+k)\beta_5\}\sinh(m-2k)h\Big] \tag{47}$$
$$\times\frac{(\beta_4-\beta_3)\sin kL}{k^2LD'}dk.$$

6. Numerical results and discussion

Eqs. (44)-(47) give the solution in the Fourier-Laplace transform domain. Two integrations are required to get the solution in the space-time domain. Schapery (1962) proposed a very simple and efficient approximate formula for finding the Laplace inversion numerically. According to this formula

$$\phi(t)=\left[s\bar{\phi}(s)\right]_{s=1/(2t)}, \tag{48}$$

where $\bar{\phi}(s)$ is the Laplace transform of $\phi(t)$. In view of its simplicity and computational efficiency, we have used Schapery's approximate formula for the Laplace inversion. Fourier transform inversion involves evaluating the semi-infinite integral with respect to k. This has been done by using the extended Simpson's rule.

We have computed the surface settlement u_3 and the pore pressure p at various points lying on the z-axis vertically below the mid point of the strip $-L \le x \le L$, $z = 0$. We introduce the following dimensionless quantities

$$P = \left(\frac{L}{\sigma_0}\right)p, \quad W = \left(\frac{G}{\sigma_0}\right)u_3(0,0),$$
$$T = \frac{2\chi_3 t}{L^2}, \qquad \gamma^2 = \frac{c_1}{c_3} = \frac{\chi_1}{\chi_3}. \tag{49}$$

First, we compare the pore pressure P and the surface settlement W for permeable and impermeable bases. Fig. 2 shows the time settlement at the mid point of the strip $-L \le x \le L$ for $\upsilon = 0.12$, $\gamma = 2$ for both permeable and impermeable bases for layer thickness $h = L$ for $\upsilon_u = 0.31$, $\alpha = 0.6$. The surface settlement is accelerated by the permeability of the base, without affecting the initial and the final settlement.

Fig. 3 shows the depth profile of pore pressure for Ruhr Sandstone in which $\upsilon = 0.12$, $\upsilon_u = 0.31$, $\alpha = 0.65$ for $T = 0.01$ at the mid point of the strip $-L \le x \le L$ for layer thickness $h = L$ and $10\,L$, for both bases. We note that the depth profiles for the two cases are significantly different for a thin stratum ($h = L$). However, for a thick stratum ($h = 10\,L$), the depth profiles for the two cases are almost identical except near the base of the stratum. Also, the pore pressure vanishes for the permeable base at the bottom of the layer, which is consistent with the boundary condition. Fig. 4 shows the diffusion of pore pressure with time for $\gamma = 0.6$ at the mid point of the strip for both permeable and impermeable bases. Near the surface, the effect of the permeability of the base is only marginal. However, near the bottom, the diffusion of the pore pressure in the two cases differs significantly.

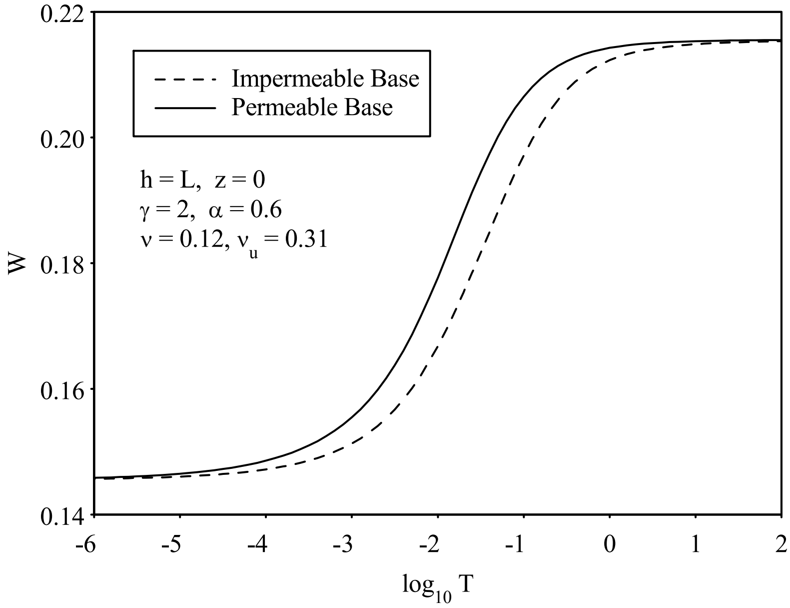

Fig. 2 Time variation of the surface settlement W (0, 0, t) at the mid point of the strip for $\upsilon = 0.12$, $\upsilon_u = 0.31$, $\alpha = 0.6$ for the layer thickness $h = L$ for both permeable and impermeable bases

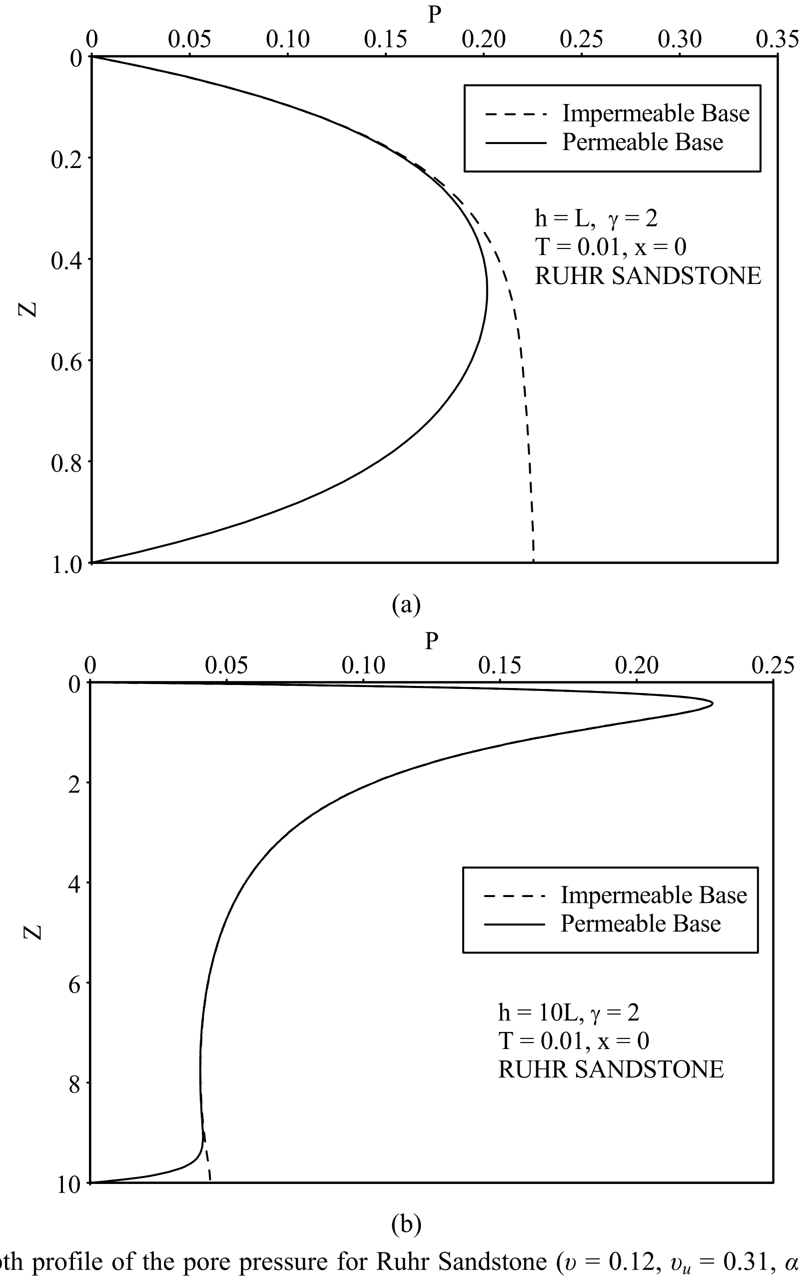

Fig. 3 Depth profile of the pore pressure for Ruhr Sandstone ($\upsilon = 0.12$, $\upsilon_u = 0.31$, $\alpha = 0.65$) for two values of layer thickness: (a) $h = L$; (b) $h = 10\ L$ for both permeable and impermeable bases

Next, we compute the pore pressure P and the surface settlement W for a permeable base. Fig. 5 shows the effect of Biot-Willis coefficient (α) on the time settlement at the mid point of the strip for $\upsilon = 0.12$, $\upsilon_u = 0.31$ and $\gamma = 2$ for layer thickness $h = L$. The coefficient α ($0 \leq \alpha \leq 1$) denotes the ratio of compressibility of the solid skeleton to the compressibility of the drained bulk material.

For incompressible solid skeleton, $\alpha = 1$. Fig. 5 indicates that the compressibility of the solid skeleton accelerates the surface settlement. The effect of undrained Poisson's ratio υ_u ($0 \leq \upsilon \leq \upsilon_u \leq 0.5$) on the surface settlement is depicted in Fig. 6 for $\upsilon = 0.12$, $\alpha = 0.65$ and $\gamma = 2$ for $h = L$.

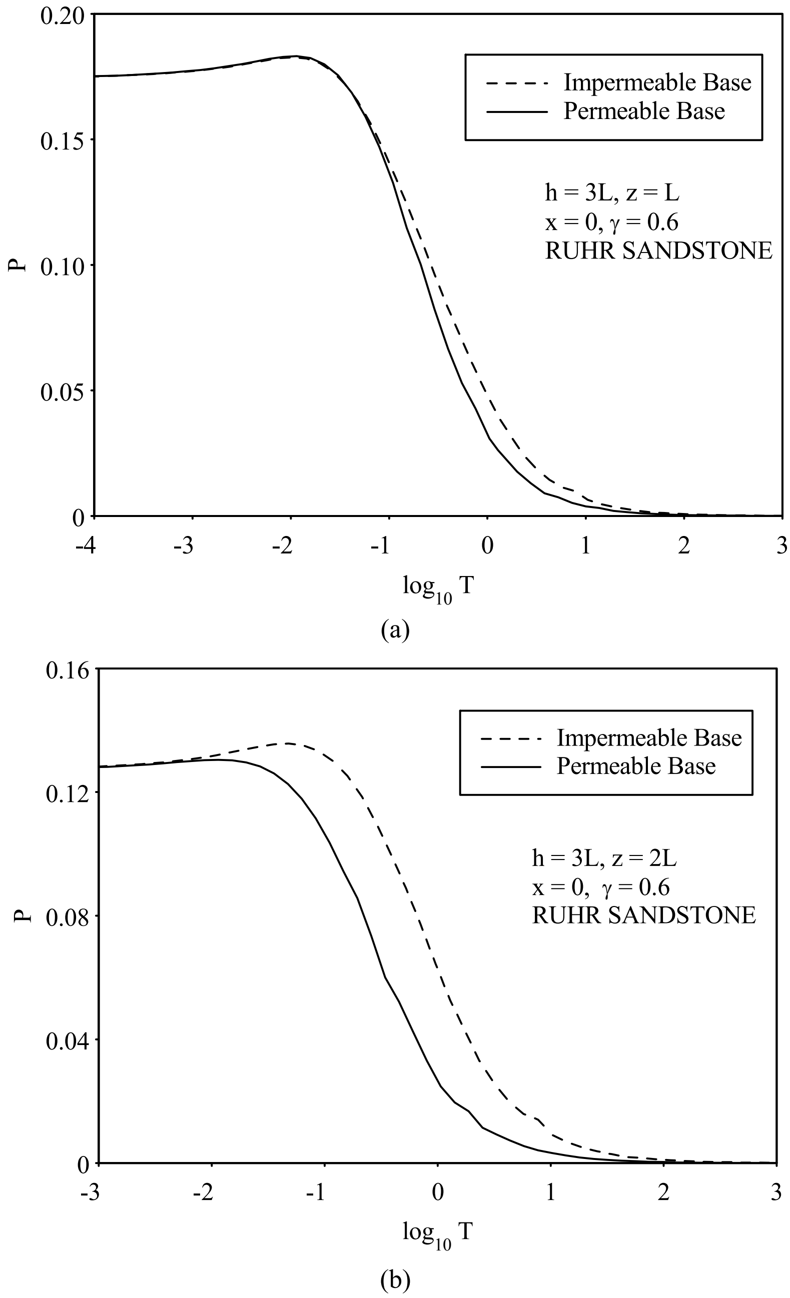

(b)

Fig. 4 Diffusion of pore pressure $P(0, z, t)$ with time for Ruhr Sandstone for (a) $z = L$; $h = 3\ L$; (b) $z = 2\ L$, $h = 3\ L$. As we approach the bottom of the layer, the permeability of base has a significant effect in pore pressure

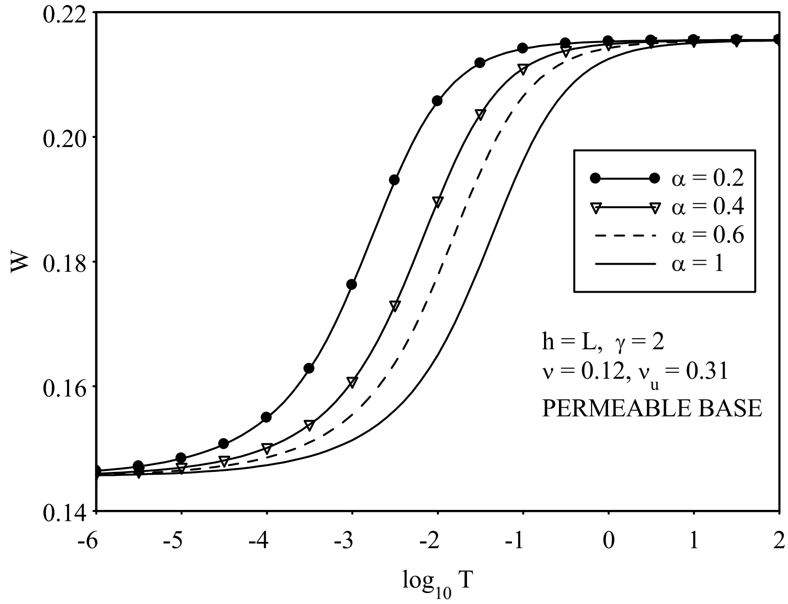

Fig. 5 Effect of the compressibility of the solid skeleton on the time settlement $W(0, 0, t)$ at the mid point of the strip for the layer thickness $h = L$

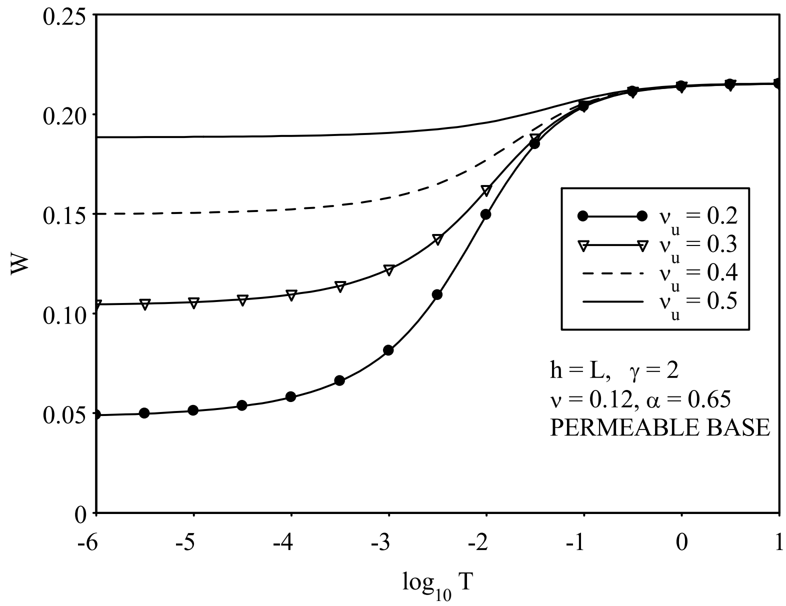

Fig. 6 Effect of the compressibility of the pore fluid on the time settlement $W(0, 0, t)$ at the mid point of the strip for $\upsilon = 0.12$, $\alpha = 0.65$ and $\gamma = 2$ for the layer thickness $h = L$

The upper limit $\upsilon_u = 0.5$ corresponds to a poroelastic material with incompressible pore fluid. The fluid constituent's compressibility increases the initial undrained settlement but has no effect on the final drained settlement.

Fig. 7 shows the effect of layer thickness on the time settlement at the mid point of the strip $-L \le x \le L$. The surface settlement increases with increase in layer thickness. Fig. 8 shows the depth profile of pore pressure for Ruhr Sandstone for which $\upsilon = 0.12$, $\upsilon_u = 0.31$, $\alpha = 0.65$ for the layer

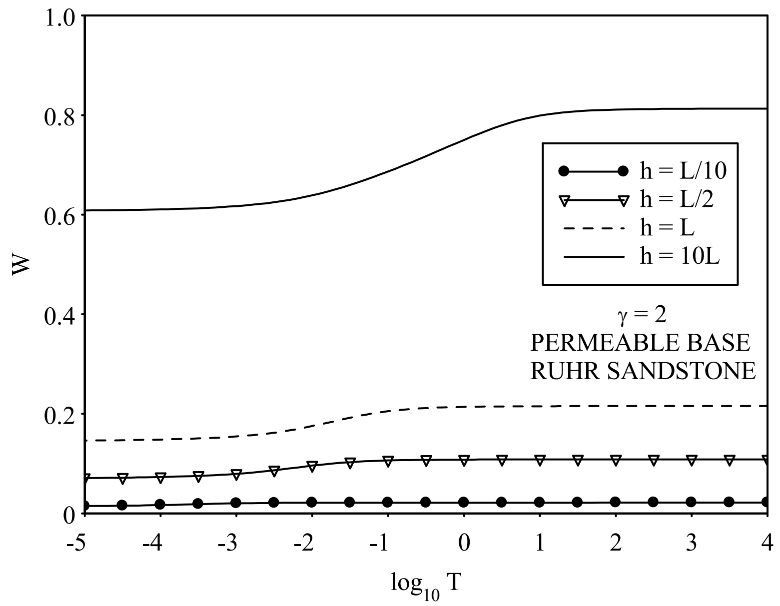

Fig. 7 Effect of the layer thickness on the settlement $W(0, 0, t)$ at the mid point of the strip for Ruhr Sandstone for $\gamma = 2$. The surface settlement increases as the layer thickness increases

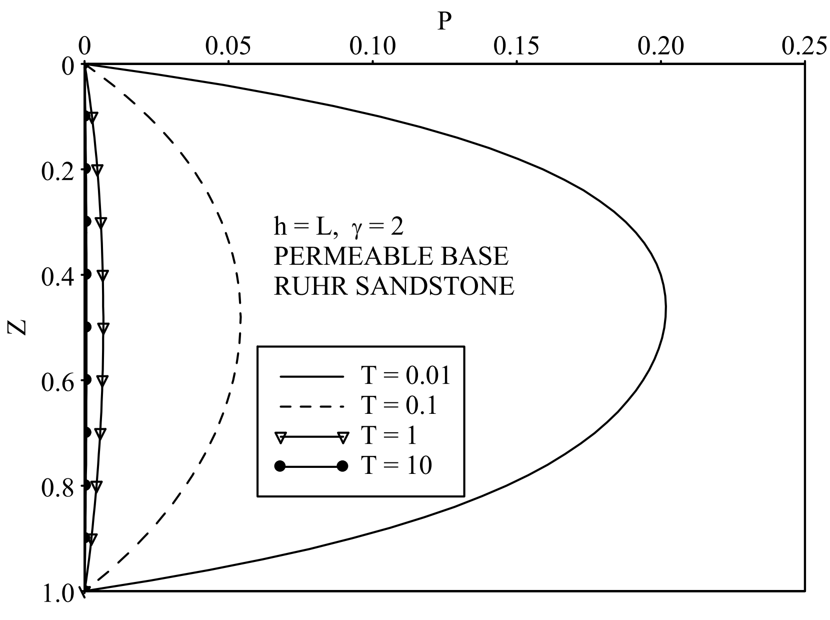

Fig. 8 Depth profile of the pore pressure $P(0, z, t)$ for Ruhr Sandstone ($\upsilon = 0.12$, $\upsilon_u = 0.31$, $\alpha = 0.65$) for the layer thickness $h = L$

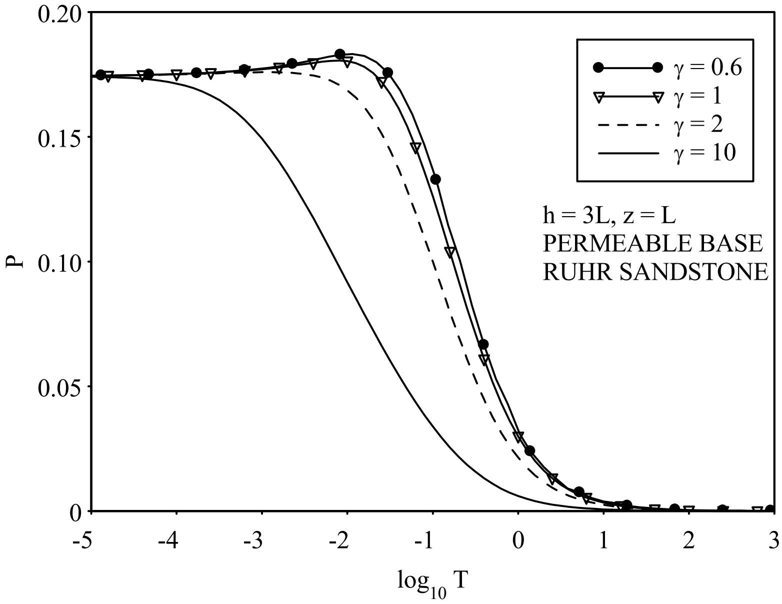

(a)

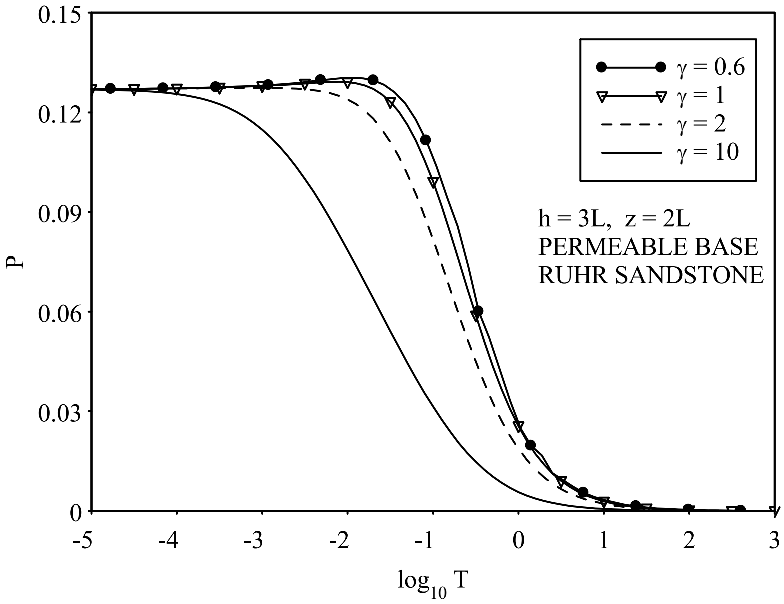

(b)

Fig. 9 Effect of the anisotropic permeability γ on the diffusion of pore pressure $P(0, z, t)$ with time for Ruhr Sandstone for (a) $z = L$, $h = 3\ L$; (b) $z = 2\ L$, $h = 3\ L$. The Mandel-Cryer effect is pronounced for small values of γ

thickness $h = L$ for different times. The pore pressure decreases with time. Fig. 9 displays the effect of anisotropic permeability on diffusion of pore pressure with time. The pore pressure rises from the initial undrained value and then decays to zero as $t \to \infty$ for small values of anisotropic parameter $\gamma = (\chi_1/\chi_3)^{1/2}$. This is the well-known Mandel-Cryer Effect. This effect is pronounced for small values of γ.

7. Conclusions

(i) The time settlement is accelerated by the permeability of the base. However, the initial and the final settlements are not affected.
(ii) Near the surface, the pore pressure is not much affected by the permeability of the base. But it has a significant effect near the bottom.
(iii) Permeability of the base affects the depth profile of the pore pressure significantly for a thin stratum. However, for a thick stratum, it does not have much effect except near the base of the stratum.
(iv) The compressibility of the solid skeleton of the poroelastic material may accelerate the consolidation process. However, it has no effect on the initial and the final settlements.
(v) The compressibility of the pore fluid increases the initial settlement. But it has no effect on the final settlement.
(vi) The surface settlement increases with an increase in the layer thickness.
(vii) The Mandel-Cryer effect of the pore pressure is more pronounced when the horizontal permeability is smaller than the vertical permeability.

Acknowledgments

The author SJS is grateful to the Indian National Science Academy for financial support under its Honorary Scientist Scheme and the author SR is thankful to UGC, New Delhi for financial support in the form of the Major Research Project. The authors thank the two referees for their useful comments.

References

Ai, Z.Y. and Wang, Q.S. (2008), "A new analytical solution to axisymmetric Biot's consolidation of a finite soil layer", *Appl. Math. Mech*., **29**(12), 1617-1624.

Ai, Z.Y. and Wu, C. (2009), "Plane strain consolidation of soil layer with anisotropic permeability", *Appl. Math. Mech*., **30**(11), 1437-1444.

Ai, Z.Y., Cheng, Z.Y. and Han, J. (2008), "State space solution to three-dimensional consolidation of multilayered soils", *Int. J. Eng. Sci.*, **46**(5), 486-498.

Ai, Z.Y., Wang, Q.S. and Han, J. (2010a), "Analytical solutions describing the consolidation of a multilayered soil under circular loading", *J. Eng. Math.*, **66**(4), 381-393.

Ai, Z.Y., Wang, Q.S. and Han, J. (2010b), "Transfer matrix solutions to axisymmetric and non-axisymmetric consolidation of multilayered soils", *Acta. Mech.*, **211**(1-2), 155-172.

Ai, Z.Y., Cheng, Y.C., Zeng, W.Z. and Wu, C. (2013), "3-D consolidation of multilayered porous medium with anisotropic permeability and compressible pore fluid", *Mecca.*, **48**(2), 491-499.

Booker, J.R. and Carter, J.P. (1986), "Long term subsidence due to fluid extraction from a saturated, anisotropic, elastic soil mass", *Q. J. Mech. Appl. Math.*, **39**(1), 85-98.

Booker, J.R. and Carter, J.P. (1987a), "Elastic consolidation around a point sink embedded in a half-space with anisotropic permeability", *Int. J. Num. Anal. Meth. Geomech*., **11**(1), 61-77.

Booker, J.R. and Carter, J.P. (1987b), "Withdrawal of a compressible pore fluid from a point sink in an isotropic elastic half-space with anisotropic permeability", *Int. J. Solids Struct*., **23**(3), 369-385.

Booker, J.R. and Randolph, M.F. (1984), "Consolidation of a cross-anisotropic soil medium", *Q. J. Mech. Appl. Math*., **37**(3), 479-495.

Chen, G.J. (2004), "Consolidation of multilayered half-space with anisotropic permeability and compressible constituents", *Int. J. Solids Struct*., **41**(16-17), 4567-4586.

Chen, G.J. (2005), "Steady-state solutions of multilayered and cross-anisotropic poroelastic half-space due to a point sink", *Int. J. Geomech*., **5**(1), 45-57.

Chen, G.J. and Gallipoli, D. (2004), "Steady infiltration from buried point source into heterogeneous cross-anisotropic unsaturated soil", *Int. J. Numer. Anal. Meth. Geomech*., **28**(10), 1033-1055.

Chen, S.L., Chen, L.Z. and Zhang, L.M. (2005a), "The axisymmetric consolidation of a semi-infinite transversely isotropic saturated soil", *Int. J. Numer. Anal. Meth. Geomech*., **29**(13), 1249-1270.

Chen, S.L., Zhang, L.M. and Chen, L.Z. (2005b), "Consolidation of a finite transversely isotropic soil layer on a rough impervious layer", *J. Eng. Mech*., **131**(12), 1279-1290.

Detournay, E. and Cheng, A.H.-D. (1993), *Fundamentals of Poroelasticity, Comprehensive Rock Engineering: Principles, Practice and Projects*, (Hudson, J.A. Ed.), Pergamon Press, Oxford, UK, Volume 2, pp. 113-171.

Ganbe, T. and Kurashige, M. (2001), "Integral equations for a 3D crack in a fluid saturated poroelastic infinite space of transversely isotropic permeability", *JSME Int. J. Ser A*., **44**(3), 423-430.

Kim, H. and Mission, J. (2011), "Numerical analysis of one-dimensional consolidation in layered clay using interface boundary relations in terms of infinitesimal strain", *Int. J. Geomech.*, **11**(1), 72-77.

Li, P., Wang, L., He, Y. and Sun, D. (2013), "An analytical solution of flow-deformation coupling due to a point sink within a finite poroelastic layer", *Proceedings of the Fifth Biot Conference on Poromechanics*, Vienna, Austria, July, pp. 541-546.

Rani, S., Kumar, R. and Singh, S.J. (2011), "Consolidation of an anisotropic compressible poroelastic clay layer by axisymmetric surface loads", *Inter. J. Geomech. ASCE*, **11**(1), 65-71.

Roeloffs, E.A. (1988), "Fault stability changes induced beneath a reservoir with cyclic variations in water level", *J. Geophys. Res.*, **93**(B3), 2107-2124.

Schapery, R.A. (1962), "Approximate method of transform inversion for viscoelastic stress analyses", *Proceedings of the 4th US National Congress on Applied Mechanics,* Berkeley, CA, USA, Volume 2, pp. 1075-1085.

Singh, S.J. and Rani, S. (2006), "Plane strain deformation of a multilayered poroelastic half-space by surface loads", *J. Earth Sys. Sci.,* **115**(6), 685-694.

Singh, S.J., Rani, S. and Kumar, R. (2007), "Quasi-static deformation of a poroelastic half-space with anisotropic permeability by two-dimensional surface loads", *Geophys. J. Int.,* **170**(3), 1311-1327.

Singh, S.J., Kumar, R. and Rani, S. (2009), "Consolidation of a poroelastic half-space with anisotropic permeability and compressible constituents by axisymmetric surface loading", *J. Earth Sys. Sci*., **118**(5), 563-574.

Taguchi, I. and Kurashige, M. (2002), "Fundamental solutions for a fluid-saturated, transversely isotropic, poroelastic solid", *Int. J. Numer. Anal. Meth. Geomech*., **26**(3), 299-321.

Wang, H.F. (2000), *Theory of Linear Poroelasticity,* Princeton University Press, Princeton, NJ, USA.

PL

Appendix

Case I: Permeable base

$$A_1 = \frac{N_0 k}{\eta D}\Big[2(m\beta_5 + \beta_4 + \beta_1)\, e^{kh} - 2(m\beta_5 - \beta_4 + \beta_2)\, e^{-kh} - 2(k\beta_5 + \beta_4)\, e^{mh} - \{\beta_6 + (m-k)\beta_5\} e^{(m+2k)h} - \{\beta_6 - (m+k)\beta_5\} e^{(m-2k)h}\Big],$$

$$A_2 = \frac{N_0 k}{\eta D}\Big[-2m\beta_5(3e^{kh} + e^{-kh}) + \{(\beta_4 - \beta_1 - \beta_2) + (3m+k)\beta_5\} e^{mh} - \{(\beta_4 - \beta_1 - \beta_2) - (3m-k)\beta_5\} e^{-mh} + \{\beta_6 + (m-k)\beta_5\} e^{(m+2k)h} - \{\beta_6 - (m+k)\beta_5\} e^{-(m-2k)h}\Big],$$

$$A_3 = \frac{N_0 k}{\eta D}\Big[2(m\beta_5 - \beta_4 - \beta_1)\, e^{kh} - 2(m\beta_5 + \beta_4 - \beta_2)\, e^{-kh} + 2(k\beta_5 + \beta_4)\, e^{-mh} + \{\beta_6 - (m+k)\beta_5\} e^{-(m-2k)h} + \{\beta_6 + (m-k)\beta_5\} e^{-(m+2k)h}\Big],$$

$$A_4 = \frac{N_0 k}{\eta D}\Big[2m\beta_5(e^{kh} + 3e^{-kh}) + \{(\beta_4 + \beta_2 + \beta_1) - (3m-k)\beta_5\} e^{mh} - \{(\beta_4 + \beta_2 + \beta_1) + (3m+k)\beta_5\} e^{-mh} + \{\beta_6 - (m+k)\beta_5\} e^{(m-2k)h} - \{\beta_6 + (m-k)\beta_5\} e^{-(m+2k)h}\Big],$$

$$\begin{aligned} B_2 = \frac{N_0}{kD}\Big[&2m\beta_5(3\beta_1 - \beta_4 - k\beta_5)\, e^{kh} + 2m\beta_5(k\beta_5 - \beta_4 + \beta_2)\, e^{-kh} \\ &+ \left\{2m\beta_5(\beta_4 - \beta_1 - \beta_2) - k\beta_5\beta_6 + \beta_1^2 + \beta_2^2 + \beta_4^2 - 2\beta_2\beta_4 + m(m-k)\beta_5^2\right\} e^{mh} \\ &+ \left\{2m\beta_5(\beta_4 - \beta_1 - \beta_2) + k\beta_5\beta_6 - \beta_1^2 - \beta_2^2 - \beta_4^2 + 2\beta_2\beta_4 - m(m+k)\beta_5^2\right\} e^{-mh} \\ &+ (\beta_4 - m\beta_5)\{\beta_6 + (m-k)\beta_5\} e^{(m+2k)h} - (\beta_4 + m\beta_5)\{\beta_6 - (m+k)\beta_5\} e^{-(m-2k)h}\Big], \end{aligned}$$

$$\begin{aligned} B_5 = \frac{N_0}{kD}\Big[&-2m\beta_5(k\beta_5 - \beta_4 - \beta_1)\, e^{kh} + 2m\beta_5(k\beta_5 + \beta_4 + 3\beta_2)\, e^{-kh} \\ &- \left\{2m\beta_5(\beta_4 + \beta_2 + \beta_1) + k\beta_5\beta_6 - \beta_1^2 - \beta_2^2 - \beta_4^2 - 2\beta_1\beta_4 - m(m+k)\beta_5^2\right\} e^{mh} \\ &- \left\{2m\beta_5(\beta_4 + \beta_2 + \beta_1) - k\beta_5\beta_6 + \beta_1^2 + \beta_2^2 + \beta_4^2 + 2\beta_1\beta_4 + m(m-k)\beta_5^2\right\} e^{-mh} \\ &+ (m\beta_5 - \beta_4)\{\beta_6 + (m-k)\beta_5\} e^{-(m+2k)h} + (m\beta_5 + \beta_4)\{\beta_6 - (m+k)\beta_5\} e^{(m-2k)h}\Big], \end{aligned}$$

where

$$s_a = s + (c_1 - c_3)k^2 = c_3(m^2 - k^2),$$

$$\beta_1 = \beta_4 kh - \beta_3, \qquad \beta_2 = \beta_4 kh + \beta_3,$$

$$\beta_3 = 1 - \frac{(1-2\upsilon)(1-\upsilon_u)s_a}{(\upsilon_u - \upsilon)s}, \quad \beta_4 = 1 + \frac{(1-\upsilon_u)s_a}{(\upsilon_u - \upsilon)s},$$

$$\beta_5 = \frac{2k}{m^2 - k^2}, \qquad \beta_6 = \beta_4 + \beta_1 - \beta_2,$$

and

$$\begin{aligned} D = {} & 8m\beta_5\left[(\beta_5 k - \beta_1)e^{kh} - (\beta_5 k + \beta_2)e^{-kh}\right] \\ & - \left[\beta_4 - (m-k)\beta_5\right]\left[\beta_6 + (m-k)\beta_5\right]\left[e^{(m+2k)h} - e^{-(m+2k)h}\right] \\ & - \left[\beta_4 + (m+k)\beta_5\right]\left[\beta_6 - (m+k)\beta_5\right]\left[e^{(m-2k)h} - e^{-(m-2k)h}\right] \\ & - 2\left[m^2\beta_5^2 + k^2\beta_5^2 + \beta_1^2 + \beta_2^2 + \beta_4^2 + (\beta_4 - k\beta_5)(\beta_1 - \beta_2) - 2m\beta_5(\beta_1 + \beta_2)\right]e^{mh} \\ & + 2\left[m^2\beta_5^2 + k^2\beta_5^2 + \beta_1^2 + \beta_2^2 + \beta_4^2 + (\beta_4 - k\beta_5)(\beta_1 - \beta_2) + 2m\beta_5(\beta_1 + \beta_2)\right]e^{-mh}. \end{aligned}$$

Case II: Impermeable base

$$\begin{aligned} A_1 = {} & \frac{N_0 k}{\eta D'}\Big[-2(m\beta_5 + \beta_2)\,e^{kh} - 2k(m\beta_5 + \beta_1)\,e^{-kh} - 2m(k\beta_5 + \beta_4)\,e^{mh} \\ & + \left\{m\beta_6 + k(m-k)\beta_5\right\}e^{(m+2k)h} + \left\{m\beta_6 + k(m+k)\beta_5\right\}e^{(m-2k)h}\Big], \end{aligned}$$

$$\begin{aligned} A_2 = {} & \frac{N_0 k}{\eta D'}\Big[2mk\beta_5(3e^{kh} - e^{-kh}) + \left\{m(\beta_1 + \beta_2 - \beta_4) - (mk + k^2 + 2m^2)\beta_5\right\}e^{mh} \\ & + \left\{m(\beta_1 + \beta_2 - \beta_4) - (mk - k^2 - 2m^2)\beta_5\right\}e^{-mh} \\ & - \left\{m\beta_6 + k(m-k)\beta_5\right\}e^{(m+2k)h} - \left\{m\beta_6 + k(m+k)\beta_5\right\}e^{-(m-2k)h}\Big], \end{aligned}$$

$$\begin{aligned} A_3 = {} & \frac{N_0 k}{\eta D'}\Big[-2k(m\beta_5 - \beta_2)\,e^{kh} - 2k(m\beta_5 - \beta_1)\,e^{-kh} + 2m(k\beta_5 + \beta_4)\,e^{-mh} \\ & + \left\{m\beta_6 + k(m+k)\beta_5\right\}e^{-(m-2k)h} + \left\{m\beta_6 + k(m-k)\beta_5\right\}e^{-(m+2k)h}\Big], \end{aligned}$$

$$A_4 = \frac{N_0 k}{\eta D'}\Big[2mk\beta_5(3e^{-kh} - e^{kh}) - \big\{m(\beta_1+\beta_2+\beta_4) + (mk - k^2 - 2m^2)\beta_5\big\}e^{mh}$$
$$- \big\{m(\beta_1+\beta_2+\beta_4) + (mk + k^2 + 2m^2)\beta_5\big\}e^{-mh}$$
$$- \big\{m\beta_6 + k(m+k)\beta_5\big\}e^{(m-2k)h} - \big\{m\beta_6 + k(m-k)\beta_5\big\}e^{-(m+2k)h}\Big],$$

$$B_2 = \frac{N_0}{kD'}\Big[2mk\beta_5(k\beta_5 - 3\beta_2 + 4\beta_4)\,e^{kh} + 2mk\beta_5(k\beta_5 + \beta_1)\,e^{-kh}$$
$$+ \big\{(\beta_1+\beta_2-\beta_4)\beta_5(m^2+k^2) - mk(\beta_6 - m\beta_5)\beta_5 - mk^2\beta_5^2$$
$$- m(\beta_1^2+\beta_2^2+\beta_4^2 - 2\beta_2\beta_4)\big\}e^{mh} - \big\{(\beta_1+\beta_2-\beta_4)\beta_5(m^2+k^2)$$
$$+ mk(\beta_6 + m\beta_5)\beta_5 + mk^2\beta_5^2 + m(\beta_1^2+\beta_2^2+\beta_4^2 - 2\beta_2\beta_4)\,e^{-mh}$$
$$+ (m\beta_5 - \beta_4)\big\{m\beta_6 + k(m-k)\beta_5\big\}e^{(m+2k)h} - (m\beta_5+\beta_4)\big\{m\beta_6 + k(m+k)\beta_5\big\}e^{-(m-2k)h}\Big],$$

$$B_5 = \frac{N_0}{kD'}\Big[2mk\beta_5(k\beta_5 - \beta_2)\,e^{kh} + 2mk\beta_5(k\beta_5 + 3\beta_1 + 4\beta_4)\,e^{-kh}$$
$$+ \big\{(\beta_1+\beta_2+\beta_4)\beta_5(m^2+k^2) - mk\beta_5(\beta_6 + m\beta_5) - mk^2\beta_5^2$$
$$- m(\beta_1^2+\beta_2^2+\beta_4^2 + 2\beta_1\beta_4)\big\}e^{mh} - \big\{(\beta_1+\beta_2+\beta_4)\beta_5(m^2+k^2)$$
$$+ mk\beta_5(\beta_6 - m\beta_5) + mk^2\beta_5^2 + m(\beta_1^2+\beta_2^2+\beta_4^2 + 2\beta_1\beta_4)\,e^{-mh}$$
$$- (m\beta_5+\beta_4)\big\{m\beta_6 + k(m+k)\beta_5\big\}e^{(m-2k)h} + (m\beta_5 - \beta_4)\big\{m\beta_6 + k(m-k)\beta_5\big\}e^{-(m+2k)h}\Big],$$

where

$$D' = 8mk\beta_5\big[(\beta_2 - \beta_4 - k\beta_5)e^{kh} - (\beta_1+\beta_4+k\beta_5)e^{-kh}\big]$$
$$+ \big[\beta_4 - (m-k)\beta_5\big]\big[m\beta_6 + k(m-k)\beta_5\big]\big[e^{(m+2k)h} + e^{-(m+2k)h}\big]$$
$$+ \big[\beta_4 + (m+k)\beta_5\big]\big[m\beta_6 + k(m+k)\beta_5\big]\big[e^{(m-2k)h} + e^{-(m-2k)h}\big]$$
$$- 2\big[\beta_5(m^2+k^2)(\beta_1+\beta_2) - mk\beta_5(\beta_4+\beta_6+2k\beta_5)\big]$$
$$- m(\beta_1^2+\beta_2^2+\beta_4^2+\beta_1\beta_4-\beta_2\beta_4)\big]e^{mh} + 2\big[\beta_5(m^2+k^2)(\beta_1+\beta_2)$$
$$+ mk\beta_5(\beta_4+\beta_6+2k\beta_5) + m(\beta_1^2+\beta_2^2+\beta_4^2+\beta_1\beta_4-\beta_2\beta_4\big]e^{-mh}\,.$$